Investigation of the Quenched Surfaces of Visibly Luminescent Macro/Nanoporous Silicon under the Exposure of Typical Neuron Culture Media

B. Unal

Departments of Computer and Software Engineering, Faculty of Engineering and Natural Sciences, Istanbul Sabahattin Zaim University, Halkali-Kucukcekmece, 34303, Istanbul, Turkey
e-mail: bayram.unal@izu.edu.tr ; bayram.unal@gmail.com

In this research paper, the quenching effects of visible photoluminescence of porous silicon relevant to doping types under an exposure of culture media such as Dulbecco's Modified Eagle's Medium and Phosphate-Buffered Saline have been studied extensively in order to realize the application of a cell culture growth technique for porous silicon, in which biocompatibility is directly based on its size-dependent structures and morphologies. This could restrain the combination of either macro- or micro-/nano-dimensional silicon morphologies by stain-etching single crystalline Si surfaces. The dopant-related quenching effect of well-known neuron culture media over visible photoluminescent porous silicon surface is found to be quite obvious for the two culture media mentioned above. Scanning electron microscope images of the cultured neuron cells over porous Si show how they have been linked to, and communicated with, each other, and directed along porous channels, fabricated by a photolithographic technique.

Keywords: porous silicon, neurons, visible photoluminescence, cell culture medium, SEM micrographs.

УДК 577/579

INTRODUCTION

Recent technological advances open up more opportunities of establishing a new communication channel between neural cell activities and nanoelectronics world [1, 2]. In the near future, mankind wishes to have a device technology to be able to replace some of non-functioned sensory organs with their hybrid bio- and nano-electronic equivalents or even visualize the construction of self-programmable or "thinkable" semi-bio-processors [3–5]. Before achieving all the concepts above, the most fundamental objective is to study interactive mechanisms of the communication between the nervous system through neuron cells and smart biomaterials being processed with a precise control of every step of fabrication. It is well-known that neurons communicate with each other by ion-exchanging signals similar to the current digital logic systems. That is the reason why it is highly desirable to investigate the interface interaction and biocompatibility between neuron cells and some "smart" biomaterials in an attempt to produce a variety of hybrid devices capable of establishing some integrated networks of the communication between biological and electronic systems [6]. One of the promising and cheap biomaterials, for example, PSi, which is a new form of the well-known electronic substrate material, has been studied to form some interfaces among such hybrid assemblies [7–9]. Hence, the culture of neuronal cells over a variety of differently modified surfaces of both nanocrystalline diamond and PSi could become a more attractive area for a new generation of biomedical application [10–12], especially for some forthcoming bio/nano-electronic interfaces for the usage of an intelligent brain-functioning system and a compact bio-computer [13, 14]. The present study is focused on one of a smart biomaterial resulting from a degree of some quenching effects over a surface of visibly-luminescent PSi layer under the exposure to the culture media, generally used for cell-culturing.

Here the experimental study covers some doping effects of visible photoluminescence (PL) originating from nano PSi layer under an exposure of well-known culture media during the cell-culturing technique for a potential application in bionano-technology [15]. This does also involve studying their destructive consequences over the structural morphologies of the nano-sized PSi surface without any buffer layer. The visible PL spectra from each of porous samples originally prepared from both *n*-and *p*-types of *c*-Si were then characterized under two different culture media after the exposure time of one- and two-hours in addition to the one with as-grown condition. The conclusive part is the investigation of the way to adhere neuron cells morphologically over a processed surface of PSi as a "smart" biocompatible material without any buffer layers at the interface [16–18].

A "SMART" BIOMATERIAL: PSi

It is currently one of the remarkable technological aims to realize a sophisticated construction and engineering configuration of some functional interfaces between PSi surfaces and living neuron cells for a wide range of biomedical applications. So, the fully-controllable production of any biocompatible nano-device and/or neural activation device for cell signaling application is one of the future aims of the author after the phenomena of neuron cells cultured *in vitro* are perfectly understood [3, 19]. This potential device is to be based on a variety of PSi surfaces, i.e. a nano-sized morphological luminescent form of macro-sized PSi, generally produced by one of such methods as an anodization or a stain-etching, or a vapor phase-etching. This is why the present work aims at clarification of types of porosity and the doping level of the porous surface that are most attractive to living neuron cells, including with a critical chemical resistance of nanoporous morphology to the cell culture media. The cultured cells used in this study are the immortalised rat hippocampal B50 neuron cells. Some cut pieces of Si wafer could be made nanoporous through a chemical stain-etching process, compatible with the current complementary metal–oxide–semiconductor technology [20–22].

EXPERIMENTAL

The production of samples was performed in two major steps with the aim so as to realise the quenching effects of visible PL of PSi under two cell-culturing media for biocompatibility. First, various types of macro-, micro- and nano-sized porosities of the processed Si surfaces were formed by the chemical stain etching of Si in an HF-based solution [23–24]. Second, porous surfaces, obtained from both *p*- and *n*-type *c*-Si substrates, have been exposed to the cell culture media such as Dulbecco's Modified Eagles Medium (DMEM) and Phosphate-Buffered Saline (PBS). Those types of culture media are also used for one of the processing steps within bio-interfacing procedures between neuron cells and microelectronic interfaces in some integrated circuit components.

Photolithography. After a standard cleaning procedure of a single c-Si wafer, a mask patterned with stripes of various widths is used for the fabrication of PSi channels to realize the manipulation of neuron cells along the fabricated channels. So, both porous and non-porous channels could be produced in order to realize the existence of the preferable lines with various widths suitable for the neuron cells analysed here.

Formation. Visibly-luminescent porous surfaces fabricated from both *p*- and *n*-type Si wafers by a simple and cost effective stain-etching technique were formed by using a new ratio of the etchant concentration between HF and HNO_3 together with ionic additives and surfactants. Both boron- and phosphorous-doped Si wafers with a resistivity range of 0.05–0.50 Ohm·cm were employed as preliminary substrates. After being cut into small square pieces of approximately 1.0 cm^2 and then being cleaned surface oxidation in a HF buffer solution, the cut pieces were prepared to be chemically stain-etched. This stain-etching process differs from the electrochemical etching process because it enables the micro- and nano-sized structural formation of porous layers without any damage in any formation of previously-manufactured components of the entire IC circuitry. For the optimisation of the stain-etch process of silicon for an efficient visible PL and the resulting porous morphology of the surfaces suitable for coherent cell culture methods, a number of experiments with various parameters have been carried out, comprising three essential steps. First, a range of the volumetric ratios of HF to HNO_3 was challenged, subsequently some of the optimal ratio was found to be either 600:1 or 800:1 for a higher PL efficiency and uniformity from the point of view of surface morphology and visibly-luminescent perspectives. Second, for the reduction of an incubation period before the initialization of actual formation of a thin porous layer during the etching process, the component $NaNO_2$ about $1g \cdot L^{-1}$ to the proposed etching solution was a good compromise. Third, an active surface agent capable of influencing the surface tension of the interface between Si surface and etching solution was explored to optimize structural surface uniformities of stain-etching [23]. Hence, the etchant solution used for this process is a chemical solution of $HF:HNO_3$ (800:1) arranged by mixing HF(48% at. wt.) and HNO_3 (70% at. wt). During stain-etching processes, both *p*- and *n*-type Si substrates were just introduced for a duration of 10 minutes under ambient illumination and room temperature. After being rinsed several times with ultra-pure millipore water, all samples were blown up with a gun of nitrogen gas to dry up porous surfaces. Quite a strong red and orange PL were observed under a UV excitation of the 325 nm wavelength selected from a He-Cd dual beam laser system. A fluorescence microscope was used to take a visible photoluminescent image from the PSi channels fabricated by a photolithographic technique.

Exposure. Some important culture media such as DMEM, suitable for the majority types of neuron cells, and a buffer solution of PBS were chosen so as to analyze their effects over visible PL emitted from

a nanostructured surface (also containing macro-porous), in which it was earlier prepared from both *p*- and *n*-type single *c*-Si pieces, since PSi is considered to be as a "smart" material for biocompatibility. These photoluminescent porous surfaces were exposed to the culture media in which they are usually widely used for cell culturing methods of B50 rat hippocampal neurons. Strong visibly-luminescent samples, cut in small squares of approximately 3x3 mm^2, have been exploited after several exposure periods of porous surfaces into cell culture media.

Spectra. First, spectral measurements were carried out for each of two dopant types of the samples named "as-prepared" surface along with an additional porous surface exposed to the cell culturing media of DMEM and PBS for a duration of one and two hours. Then, the spectrum analysis of the resulting samples has been made in the visible range by measuring the emitted light under an excitation wavelength of the UV line 325 nm of dual beam He-Cd laser. PL measurement setup contains the followings: (1) a dual He:Cd laser lined with a UV-325 nm, and Blue-442 nm, (2) transfer of a laser beam by an optic fibre, (3) a sampling holder stage for positioning, (4) a monochromator and photodetector/photomultiplier, (5) long pass filters used along laser line to cut off second harmonics (also the incident angle was tuned to get rid of the back-reflection of second harmonics (~ 650 nm), (6) a computer-controlled data collection system including an analysis software. System correction has also been paid attention to when obtaining luminescence spectra from both treated and untreated PSi surfaces.

RESULTS AND DISCUSSIONS

Efficient red and orange photoluminescent stripes of PSi fabricated by the proposed by the author novel stain-etching methods after a standard photolithographic process are illustrated in Fig. 1, respectively. Glowing microscopic images have been taken from a fluorescence microscope under a UV excitation together with a high pass filter to cut UV excitation components in the emission side of the setup. The width of each stripe is about 100 μm, suitable in size for culturing neuron cells along each of the channelled porous surfaces.

It is in line with one of the aims of the present study – to associate bidirectional interactions between the realistic physical morphologies of direct size-dependent "smart" porous structures without any buffer interfacial layer and the neuron cells to be cultured and fixed by means of two culture media over porous surfaces.

Another aim was to determine the morphological dependencies of porous structures over both doping types, which have already been fabricated from single *c*-Si substrates, and the cultured media used for dispensing the immortalised rat hippocampus B50 neuron cells. Surface morphologies after cell culturing processes have been examined by (i) both relative attenuations of the quantum efficiency and the spectral energy shifts of visible PL spectra, and (ii) the surface micrographs of the scanning electron microscope (SEM). Furthermore, some of neural cells studied here were also investigated in order to understand how their biocompatibility has been developed.

The quenching effect of PL of PSi has been extensively examined on a relative quantum efficiency and emission energy-shift for a variety of stain-etched PSi surfaces originally fabricated from both *p* (*Boron*)- and *n* (*Phosphorous*)-type *c*-Si<100> wafers with a measured resistivity of 0.5 Ohm·cm by exposing to the well-known culture media such as DMEM and PBS as shown in Fig. 2a–d. Both as-grown and the exposed samples with a duration of one and two hours were chosen to observe their variations in emission quantum efficiency, emission energy, and surface morphologies, as can be developed for a requested modification as a set of promising smart biomaterials used for any type of bio-adapted compact devices in nanoelectronics technology.

The quenching influence of DMEM and PBS culture media over visible PL spectral ranges can usually play an important role that varies depending on the doping type and the initial form of single *c*-Si substrates. This process causes a verification of individually-visible glowing nano-centers, with a dependency of quenching rates of the alkaline hydroxyls within culture media on dopant types of the material. Figures 2a and c show that under the exposure to DMEM, the quenching effects of visible PL spectra from both *n*- and *p*-types PSi seem decreasing with culturing duration for one hour and two hours when compared with those of non-exposed porous surfaces. It is clearly seen that the quenching degree of the alkaline hydroxyls in culture media is the determinant in etching away the active porous layer (*thickness reduction*), rather than etching mechanisms that reduce the effective size of the nanostructures, indicative of visible emission spectra. It is also worth noting that the degradation ratio of PL of the *p*-type PSi surface is found to be smaller than that of the *n*-type counterpart. That is, the peak wavelength of emission of the *p*-type PSi after the exposure to DMEM for two hours illustrates a red-shift to a value of 652{660}nm from 645{646}nm (total red-shift=7{14}nm) while that of the *n*-type is blue-shifted to a value of 595{607}nm from 651{660}nm (total blue-shift=56{53}nm). So, the DMEM exposure causes a red-shift for *p*-type PSi and a blue-shift for *n*-type counterpart. This means that the band-gap broade-

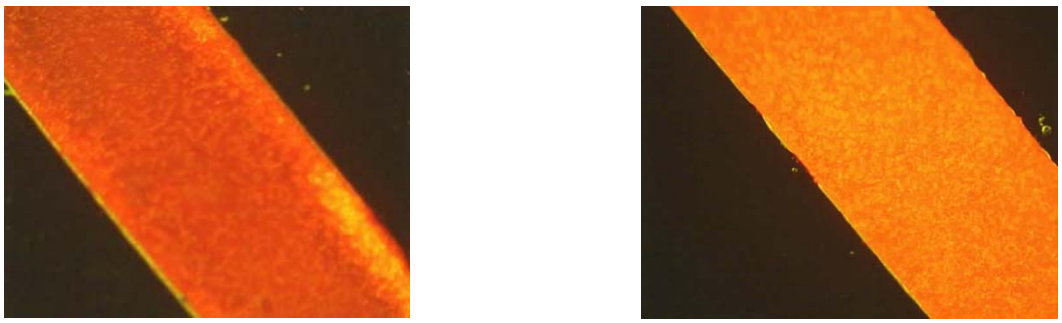

(a) (b)

Fig. 1. (a) Red and (b) orange photoluminescent stripes of PSi fabricated after a standard photolithographic process. Images have been taken from a fluorescence microscope under a UV excitation. The width of each stripe is about 100 microns suitable for culturing neuron cells along it.

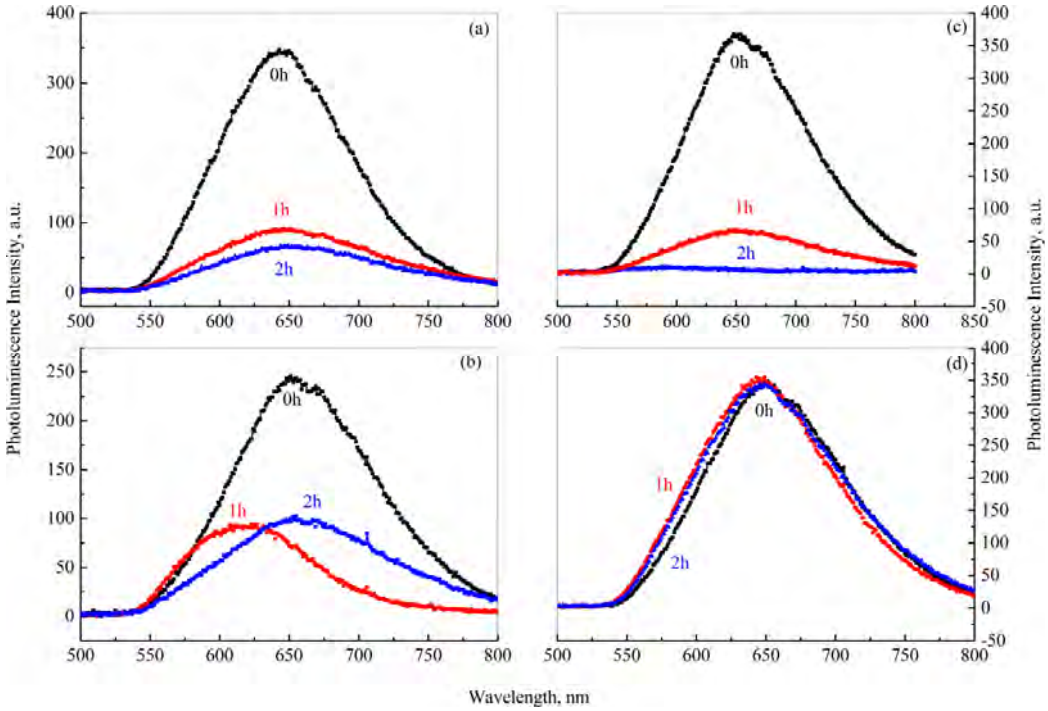

Fig. 2. Quenching effect of PL of (a) *p*-type PSi exposed to DMEM for 0, 1, and 2hrs; (b) *p*-type PSi exposed to PBS for 0, 1, and 2hrs; (c) *n*-type PSi exposed to DMEM for 0, 1, and 2hrs; and (d) *n*-type PSi exposed to PBS for 0, 1, and 2hrs.

ning occurs due to the quantum confinement size effect so that the dimension of the original nanostructure becomes narrower. The dimensionality percentage of the size distribution for the DMEM exposure of *p*-type PSi is calculated to be an increase of 32% while that for the DMEM exposure of n-type one is reduced by about 3%.

Figure 2b demonstrates that the quenching effect of visible PL spectra during PBS exposure is observed only for *p*-type PSi, in which its intensity is clearly reduced with PBS exposure when compared with those of *n*-type PSi surface as in Fig. 2d. It is undoubtedly note that the quenching measure is again rather predominant by etching away the active luminescent porous layer resulting in thickness reduction, in addition to a little complicated etching mechanism by either reducing or increasing the relative nano pillar dimensionalities against original pillar size of unexposed PSi. So "reducing" causes *blue-shifted PL* while "increasing" results in *red-shifted one*. In other words, after exposure of one hour, a blue-shifted PL is observed, and after two hours the red-shifted PL is seen explicitly with a huge shift to the red side. However, during the first hour of exposure to PBS of the *p*-type PSi, the blue-shift to a value of 657{661}nm from 618{622}nm (total blue shift=39{39}nm) is observed with a tremendous reduction in PL efficiency. In addition, during the further exposure time interval of 1hrs {totally 2hrs}, the red-shifted PL is observed at the wavelength back to 657{663}nm from 618{622}nm (total red-shift=39{41}nm). It is also interesting to note that a further exposure duration of the *p*-type PSi to PBS results in no significant changes in the PL efficiency, while the band-gap broadening and narrowing, due to quantum confinement size effects, are a good promise to understand the mechanisms of the quenching effect related to the original doping type. The dimensionality percentage of the size

Table. Full Width Half Maximum (FWHM) and peak values of PL of quenched PSi with both PBS and DMEM cell culture media for as prepared, 1,0hr, and 2,0hrs exposer time (where $\lambda_{center} = \lambda_{min} + \frac{1}{2}\lambda_{FWHM}$ and $\lambda_{shift} = \lambda_{center} - \lambda_{peak}$)

Samples	Culture Media	Exposed Time (hrs)	λ_{min} (nm)	λ_{max} (nm)	λ_{FWHM} (nm)	λ_{peak} (nm)	λ_{center} (nm)	λ_{shift} (nm)
P-type PSi	PBS	0	601	721	120	657	661,0	4,0
		1	566	678	112	618	622,0	4,0
		2	592	734	142	657	663,0	6,0
	DMEM	0	590	701	111	645	645,5	0,5
		1	583	729	146	647	656,0	9,0
		2	586	733	147	652	659,5	7,5
N-type PSi	PBS	0	599	714	115	650	656,5	6,5
		1	589	707	118	645	648,0	3,0
		2	591	714	123	647	652,5	5,5
	DMEM	0	600	720	120	651	660,0	9,0
		1	585	737	152	650	661,0	11,0
		2	548	665	117	595	606,5	11,5

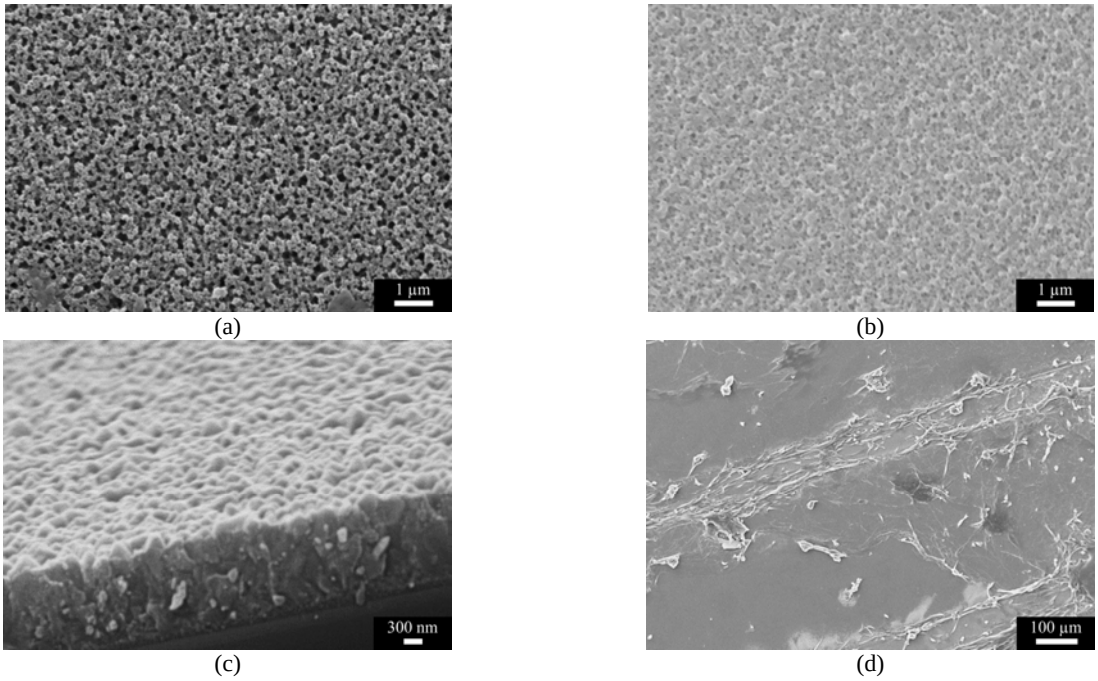

Fig. 3. SEM micrographs of (a) PSi surface (b) cultured media processed PS surface (c) cross-sectional PSi and (d) PSi-channelled surfaces cultured with several B50 hippocampal neurons. Initial wafer was a single crystalline Si (100) with a resistivity of approx 0.12 Ohm·cm.

distribution for one-hr-PBS exposure of *p*-type sample has been calculated to be reduced by 7% while that for two-hrs-PBS exposure of *n*-type one increased by about 18%. Figure 2d illustrates PL spectra of *n*-type PSi exposed to PBS for one and two-hrs, as well as of non-exposed original sample used as a reference curve. It is clearly seen that there is no significant variation in any PL spectra either for the efficiency or the energy shift of the emission, which means that there is no significant quenching effect on *n*-type PSi exposed to PBS. The dimensionality percentage of *n*-type PSi was calculated with an increase of about 7% for a PBS exposure, and the amount of wavelength of blue-shifted emission is found to be about 3–4 nm. These are summarized in the Table.

SEM micrographs of the surface morphology of micro-sized PSi before and after some standard exposure period of the culture media can be clearly visualised in Fig. 3a and b, respectively. Additionally, its cross-sectional micrograph as in Fig. 3c represents the thickness of porous layer after cell-culture processes. Principally micro-sized PSi layer remains almost unchanged, and however, visible emission of thinner nanostructured layer grown over thick microporous surfaces seems to quench as an indication of reduction of PL intensity. Actually, since microporous layer (morphological feature sizes larger than 5 nm) of a film thickness of around 1 μm becomes non-luminescent within the visible region while relatively thinner nano-sized PSi layer, especially less than 5 nm in feature sizes of some different morphology, leads to visible emission spectra. To realize biocompatibility of PSi, some porous channels over single *c*-Si wafers

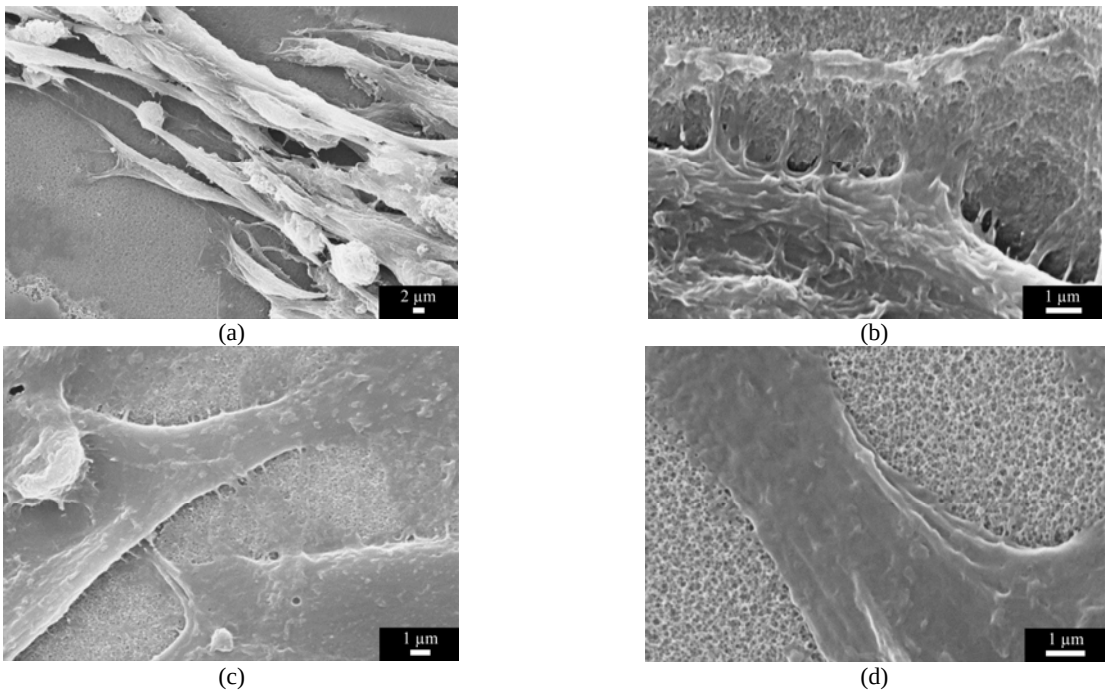

(a) (b) (c) (d)

Fig. 4. SEM micrographs of (a) several B50 hippocampal neuron cells fixed over the surface of a PSi channel (b) the nerve cell adhesion to a sidewall surface of porous channel (c and d). A cultured neuron cell and its biocompatibility using visible luminescent and non-luminescent PSi, respectively. Initial wafer was a single *c*-Si <100> with a resistivity of approximately 0.12 Ohm·cm.

have been fabricated by using a standard photolithographic technique to comprehend the size-dependent biocompatibility between porous and non-porous layers as depicted in Fig. 3d. On the other hand, micro-sized PSi layer has an indication observed clearly in the relevant SEM image given while the existence of silicon nanostructures less than 5 nm in feature size is the indication of visible emission from stain-etched PSi surface because of the theory of quantum confinement size effects. So, it is apparent to note that the cultured neuron cells follow along PSi channels as illustrated in Fig. 3d. This gives us some opportunity to manipulate neuron cells by means of any topography of the required patterns to be bio-engineered for a near future nanotechnology assisted bioelectronics devices.

Some SEM micrographs of several B50 rat hippocampal neuron cells cultured and then fixed over channelled PSi surfaces generated via a standard lithographic process are shown in Fig. 4. To have porous channels for cell culturing, a variety of stripes with different widths after photolitho-graphic steps could be investigated before stain etching. It can be stated that neuron cells prefer to grow over porous surface, therefore they could be directed along the patterned porous channels as indicated in Fig. 3d, and magnified in Fig. 4a. Since neuron cells are well-known to be electrically excitable cells that process and transmit information by means of electrical and chemical signals, the level of the connectivity and manipulation among neuron cells becomes very important through some structural modifications of porous channels as a consequence of their biocompatibility features. Fig. 4b demonstrates the adhesion of neuron cells to the sidewall of a porous channel, in which the size of pores seems to be relatively rougher when compared with the plane surface of channels. Close approaches to the processed porous surfaces indicate that specialized connections with other cells – a strong adhesion of neuron cells attached onto porous surface through some dendrites and synapses – are the base for understanding biocompatibility mechanisms and even penetration of some dendrites and synapses of the cells into pores, as illustrated in Fig. 4c and d. In order to comprehend and improve the degree of biocompatibility, more detailed research should be done in this field by studying some more parameters, especially used for some future bio-computing applications. The sidewall adhesion of some dendrites or synapses of neurons is also found to be interesting. Note that some more precaution is needed during the fabrication steps of porous channels due to the excess porous level changes of the original layer. Accordingly, a channel levelling problem results from production influences of some parameter during “etching away” and subsequently “quenching”. Finally, no passivation layer has been applied over porous surfaces during the culturing period of neurons as opposed to the one used in ref. [25]. In addition to above discussion, it is important to realize that a fused silica substrate gives less biocompatibility than in case of single crystalline silicon, however, oxygen and hydrogen terminating nanocrystalline diamond surfaces seem

to have a good adhesion after the growth of neuroblastoma cells in a perspective of chemical bonding aspects [10]. In this study, visibly-luminescent nanostructured porous surfaces, as physical morphological aspects, show a high biocompatibility for the immortalised rat hippocampus B50 neuron cells together with the controlling of the surface morphology under dopant levels of *c*-Si substrate.

CONCLUSIONS

To conclude, the quenching effects of visible PL of a controllable "smart" biomaterial such as PSi have been studied extensively since its biocompatibility to neuron cells cultured into the mostly preferable culture media of DMEM and PBS is realised. It is clear that the nanoporous surface modification of silicon as an indication of the quenching effect of visible PL in some aspects depends on an innovative dopant type of the preliminary silicon wafers. It is interesting to note that visible PL of *n*-type PSi exposed as-prepared, to PBS for one and two-hrs, has no significant modifications while the rest demonstrates some significant changes in both efficiency and energy shift of their visible emissions as either red- or blue-shift in a complicated manner. So the PL dependency of the dopants on the cell culture media was found to be quite crucial and, therefore, characterised as functions of both visible PL and the morphological correlation between nano-sized PSi and B50 rat hippocampal neuron cells. Additionally, some SEM images shows how B50 neuron cells have penetrated into pores, thus making good adhesion for biocompatibility; also it is shown that they prefer to line up along porous channels fabricated by a photolithographic method.

ACKNOWLEDGEMENTS

The author expresses his gratitude to Mrs Amanda Charalambou and Mr. C. Durand for assistance in cell culturing processes, and to Dr. A.V. Sapelkin for discussions.

REFERENCES

1. Agrawal A.A., Nehilla B.J., Reisig K.V., Gaborski T.R., Fang D.Z., Striemer C.C., Fauchet P.M., Mc Grath J.L. Porous Nanocrystalline Silicon Membranes as Highly Permeable and Molecularly thin Substrates for Cell Culture. *Biomaterials.* 2010, **31**, 5408–5417.
2. Kilian K.A., Magenau A., Böcking T., Gaus K., Gal M., Gooding J.J. Silicon-based Mesoporous Photonic Crystals: Towards Single Cell Optical Biosensors. *Proc. of SPIE*. 2009, **7397**, 739703–1.
3. Sapelkin A.V., Bayliss S.C., Unal B., Charalambou A. Interaction of B50 Rat Hippocampal Cells with Stain-etched Porous Silicon. *Biomaterials.* 2006, **27**(6), 842–846.
4. Ben-Tabou de-Leon S., Oren R., Spira M.E., Korbakov N., Yitzchaik S. and Sa'ar A. Porous Silicon Substrates for Neurons Culturing and Bio-photonic Sensing. *Phys Stat Sol A*. 2005, **202**(8), 1456–1461.
5. Braun D., Fromherz P. Fluorescence Interferometry of Neuronal Cell Adhesion on Microstructured Silicon. *Phys Rev Lett.* 1998, **8**(23), 5241–5244.
6. Frewin C.L. The Neuron-silicon Carbide Interface: Biocompatibility Study and BMI Device Development. *Theses and Dissertations Graduate School of University of South Florida*, *PhD.Thesis*, 2009. *http://scholarcommons.usf.edu/etd/1973*
7. Alvarez S.D., Derfus A.M., Schwartz M.P., Bhatia S.N., Sailor M.J. The Compatibility of Hepatocytes with Chemically Modified Porous Silicon with Reference to in Vitro Biosensors. *Biomaterials*. 2009, **30**, 26–34.
8. Bayliss S.C., Buckberry L.D., Harris P.J. and Tobin M. Nature of the Silicon-Animal Cell Interface. *J Porous Mat.* 2000, **7**, 191–195.
9. Bayliss S.C., Ashraf I., Sapelkin A.V. Concerning Signaling in *in Vitro* Neural Arrays Using Porous Silicon. *Front Multifunct Integ Nanosyst.* 2005, **152**, 467–471.
10. Vaitkuviene A., McDonald M., Vahidpour F., Noben J.-P., Sanen K., Ameloot M., Ratautaite V., Kaseta V., Biziuleviciene G., Ramanaviciene A., Nesladek M., Ramanavicius A. Impact of Differently Modified Nanocrystalline Diamond on the Growth of Neuroblastoma Cells. *New Biotechnology.* 2015, **32**(1), 7–12.
11. Salonen J., Lehto V.-P. Fabrication and Chemical Surface Modification of Mesoporous Silicon for Biomedical Applications. *Chem Eng J.* 2008, **137**, 162–172.
12. Ghaemi S.R., Harding F.J., Delalat B., Gronthos S., Voelcker N.H. Exploring the Mesenchymal Stem Cell Niche Using High Throughput Screening. *Biomaterials.* 2013, **34**, 7601–7615.
13. Punzon Q.E., Sanchez V.V., Munoz N.A., Perez R.M.J., Martin P.R.J. Nanostructured Porous Silicon Micropatterns as a Tool for Substrate-conditioned Cell Research. *Nanoscale Research Letters.* 2012, **7**, 396 (1–7).
14. Mayne A.H., Bayliss S.C., Barr P., Tobin M., Buckberry L.D. Biologically Interfaced Porous Silicon Devices. *Phys Status Solidi A.* 2000, **182**, 505–513.
15. Torres-Costa V., Martínez-Muñoz G., Sánchez-Vaquero V., Muñoz-Noval Á., González-Méndez L., Punzón-Quijorna E., Gallach-Pérez D., Manso-Silván M., Climent-Font A., García-Ruiz J.P., Martín-Palma R.J. Engineering of Silicon Surfaces at the Micro- and Nanoscales for Cell Adhesion and Migration Control. *International J. of Nanomedicine.* 2012, **7**, 623–630.

16. Fan Y.W., Cui F.Z., Hou S.P., Xu Q.Y., Chen L.N., Lee I.-S. Culture of Neural Cells on Silicon Wafers with Nano-scale Surface Topograph. *J Neurosci Meth.* 2002, **120**, 17–23.

17. Bonanno L.M., DeLouise L.A. Whole Blood Optical Biosensor. *Biosens Bioelectron.* 2007, **23**(3), 444–448.

18. Low S.P., Williams K.A., Canham L.T., Voelcker N.H. Evaluation of Mammalian Cell Adhesion on Surface-modified Porous Silicon. *Biomaterials.* 2006, **27**, 4538–4546.

19. Balasubramaniama S., Boyle N.T., Della-Chiesa A., Walsha F., Mardinoglu A., Botvich D., Prina-Mello A. Development of Artificial Neuronal Networks for Molecular Communication. *NanoCommunication Networks*. 2011, **2**, 150–160.

20. Kotzar G., Freas M., Abel P., Fleischman A., Roy S., Zorman C., Moran J.M., Melzak J. Evaluation of MEMS Materials of Construction for Implantable Medical Devices. *Biomaterials.* 2002, **23**, 2737–2750.

21. Cyster L.A., Parker K.G., Parker T.L., Grant D.M. The Effect of Surface Chemistry and Nanotopography of Titanium Nitride (TiN) Films on Primary Hippocampal Neurons. *Biomaterials.* 2004, **25**(1), 97–107.

22. Unal B. Quenching Influence of Cell Culture Medium on Photoluminescence and Morphological Structure of Porous Silicon. *Appl Sur Sci.* 2011, **258**(1), 207–211.

23. Unal B., Parbukov A.N., Bayliss S.C. Photovoltaic Properties of a Novel Stain Etched Porous Silicon and its Application in Photosensitive Devices. *Opt Mater*. 2001, **17**(1–2), 79–82.

24. Vazsonyi E., Szilagyib E., Petrika P., Horvatha Z.E., Lohner T., Frieda M., Jalsovszky G. Porous Silicon Formation by Stain Etching Thin Solid Films 2001, **388**, 295–302.

25. Ben-Tabou de Leon S., Sa'ar A., Oren R., Spira M.E., Yitzchaik S. Neurons Culturing and Biophotonic Sensing Using Porous Silicon. *Appl Phys Lett.* 2004, **84**(22), 4361–4363.

Received 01.10.14
Accepted 01.12.14

Реферат

Эффекты тушения видимой фотолюминесценции пористого кремния, относящейся к типам легирующих под воздействием культуральных сред, таких как среда Игла модифицированная Дульбекко и фосфатно-солевого буфера были широко изучены, чтобы реализовать применение метода выращивания клеточной культуры для пористого кремния, в котором биологическая совместимость непосредственно базируется на ее размерно-зависимых структурах и морфологии. Это может сдерживать образование сочетания либо макро- или микро-/наномерных кремниевых морфологий окрашивающим травления поверхностей монокристаллического Si. Эффект тушения, обусловленный наличием легирующей примеси в хорошо известной культуральной среде для нейронов, на заметно фотолюминесцентной пористой поверхности кремния также отчётливо проявляется для двух упомянутых выше питательных сред. Методом сканирующей электронной микроскопии культивируемых нейронных клеток на пористом кремнии показано, как они были связаны между собой и как сообщаются друг с другом, и направлены вдоль пористых каналов, полученных методом фотолитографии.

Ключевые слова: пористый кремний, нейроны, видимая фотолюминесценция, среда клеточных культур, СЭМ-микрофотография.